

## Supporting Information

### Exploration and optimization of the polymer-modified NiO<sub>x</sub> hole transport layer for fabricating inverted perovskite solar cells

You-Wei Wu, Ching-Ying Wang and Sheng-Hsiung Yang\*

*Institute of Lighting and Energy Photonics, College of Photonics, National Yang Ming Chiao Tung University, No.301, Section 2, Gaofa 3<sup>rd</sup> Road, Guiren District, Tainan 711010, Taiwan R.O.C.*

\*Correspondence: [yangsh@nycu.edu.tw](mailto:yangsh@nycu.edu.tw)

#### Experimental section

##### 1. Materials

The FTO-coated glass substrates were bought from Ruilong Optoelectronics Technology Co., Ltd. PVB and tetrabutylammonium tetrafluoroborate (TBABF<sub>4</sub>, purity 98%) were purchased from Vetec and Acros, respectively. Nickel acetate tetrahydrate (purity 98+%), ethanolamine (purity 99%) and high-quality perovskite precursors including lead bromide (PbBr<sub>2</sub>, purity 99.99%), lead iodide (PbI<sub>2</sub>, purity 99.9985%) and cesium iodide (CsI, purity 99.9%) were all bought from Alfa Aesar. Formamidinium iodide (FAI, purity 98%) and methylammonium bromide (MABr, purity 98%) were acquired from STAREK Scientific Co. Ltd. and TCI, respectively. [6,6]-Phenyl-C<sub>61</sub>-butyric acid methyl ester (PC<sub>61</sub>BM, purity 99%) and polyethyleneimine (PEI, molecular weight 25,000 g/mol) were obtained from Solenne B. V. and Sigma-Aldrich, respectively. Other solvents were acquired from Alfa Aesar or Acros and utilized without additional purification.

## 2. Preparation of perovskite layers

The composition of the perovskite in this research is  $\text{Cs}_{0.05}\text{FA}_{0.81}\text{MA}_{0.14}\text{Pb}(\text{Br}_{0.15}\text{I}_{0.85})_3$ . To prepare the precursor solution, a mixture of MABr (21.8 mg),  $\text{PbBr}_2$  (77.1 mg), FAI (190.2 mg),  $\text{PbI}_2$  (548.6 mg), and CsI (17.5 mg) in 1 mL of a mixed solvent composed of *N,N*-dimethylformamide (DMF) and dimethyl sulfoxide (DMSO) with 4:1 volume ratio was heated at 70 °C with stirring in a sealed glass vial for 1 hour, followed by filtration with 0.22  $\mu\text{m}$  PTFE filters. The perovskite precursor solution was spin coated into thin films in a nitrogen-filled glovebox in two steps: the first step was set at 1200 rpm for 10 s and the second step was set at 4500 rpm for 20 s. During the second step, 300  $\mu\text{L}$  of ethyl acetate was dripped on the spinning substrate. The deposited thin film was then annealed at 105 °C for 1 hour to obtain a dark brown perovskite layer.

## 3. Device fabrication

The device structure of PSCs in this study is FTO/o- $\text{NiO}_x$ , p- $\text{NiO}_x$ , or p- $\text{NiO}_x$ /o- $\text{NiO}_x$ /perovskite/ $\text{PC}_{61}\text{BM}+\text{TBABF}_4$ /PEI/Ag. FTO-coated glass substrates were cleaned in advance in detergent, deionized water, acetone, and isopropanol (IPA) for 10 min each under ultra-sonication, followed by UV-ozone exposure for 25 min. After depositing  $\text{NiO}_x$  and perovskite layers, the  $\text{PC}_{61}\text{BM}$  solution (20 mg  $\text{mL}^{-1}$ ) containing 2 mol% of  $\text{TBABF}_4$  in chlorobenzene was spin-coated on the perovskite layer at 3000 rpm for 30 s, followed by heating at 100 °C for 10 min. 0.1 mol% of PEI in anhydrous IPA was then spin-coated on the PCBM layer at 5000 rpm for 30 s. Finally, 100 nm of Ag electrodes were deposited by thermal evaporation at a base pressure of  $6 \times 10^{-6}$  torr. The active area of each device was defined by a shadow mask with an open

area of 4.5 mm<sup>2</sup>. Besides, hole-only devices with the configuration of FTO/o-NiO<sub>x</sub>, p-NiO<sub>x</sub>, or p-NiO<sub>x</sub>/o-NiO<sub>x</sub>/Ag were fabricated and their current–voltage (*I–V*) characteristics were measured for comparison.

#### 4. Characterization

*Characterization of o-NiO<sub>x</sub> and p-NiO<sub>x</sub> films.* The current–voltage (*I–V*) characteristics of hole-only devices were tested by using a Keithley 2400 source meter. The absorption and transmission spectra of specimens were measured by a Princeton Instruments Acton 2150 spectrophotometer, using a Xenon lamp as the light source (ABET Technologies LS 150). X-ray photoelectron spectroscopy (XPS) measurements were implemented by a Thermo Scientific K-Alpha spectrometer for elemental composition determination of o-NiO<sub>x</sub> and p-NiO<sub>x</sub> films. Ultraviolet photoelectron spectroscopy (UPS) measurements for different NiO<sub>x</sub> HTLs were executed on a Thermo VG-Scientific/Sigma Probe spectrometer. He I ( $h\nu = 21.22$  eV) discharge lamp was used as the excitation source. The top-view morphologies of samples were observed with an ultrahigh resolution ZEISS AURIGA Crossbeam scanning electron microscope (SEM). The surface morphology and roughness of different NiO<sub>x</sub> films were measured by a Bruker Innova atomic force microscope (AFM). The X-ray diffraction (XRD) patterns and crystallinity were characterized by a Rigaku D/MAX2500 X-ray diffractometer.

*Investigation of the Perovskite layer.* Top-view SEM images were observed with an ultrahigh-resolution ZEISS AURIGA Crossbeam SEM. The steady-state photoluminescence (PL) were acquired by using an Oxford Instruments ANDOR Kymera 193i-B1 spectrometer. An Omicron QuixX 473-100 PS laser with an excitation wavelength at 473 nm was utilized as the light source. To perform time-

resolved PL (TR-PL) measurements, a 473 nm pulsed laser (Omicron) was utilized as an excitation light source. The TR-PL signals were recorded by a time-correlated single-photon counting module (PicoQuant MultiHarp 150 4N) combined with a photomultiplier tube through an Andor Kymera 328i spectrometer.

*Evaluation of solar devices.* The current density–voltage (J–V) characteristics of PSCs were gauged using a Keithley 2400 source meter under AM 1.5G simulated sunlight exposure (Yamashita Denso YSS-100A equipped with a Xenon Short Arc lamp 1000W) at 100 mW/cm<sup>2</sup> in ambient environment. The dark current measurement of PSCs was performed using the same source meter in the dark environment. The external quantum efficiency (EQE) spectra were measured by a PV Measurement QE-R instrument.

Table S1. Lifetime parameters of TR-PL curves of the perovskite on the FTO substrate, o-NiO<sub>x</sub>, p-NiO<sub>x</sub>, and p-NiO<sub>x</sub>/o-NiO<sub>x</sub> structure.

substrate	A <sub>1</sub> (%)	τ <sub>1</sub> (ns)	A <sub>2</sub> (%)	τ <sub>2</sub> (ns)	τ <sub>avg</sub> (ns)
<b>FTO</b>	41.2	16.60	58.7	96.64	84.14
<b>o-NiO<sub>x</sub></b>	57.5	11.12	42.4	54.68	45.25
<b>p-NiO<sub>x</sub></b>	57.7	9.50	42.3	62.81	53.73
<b>p-NiO<sub>x</sub>/o-NiO<sub>x</sub></b>	50.8	9.04	49.1	36.76	31.15

Table S2. Device performance of inverted PSCs based on the o-NiO<sub>x</sub>, p-NiO<sub>x</sub> and p-NiO<sub>x</sub>/o-NiO<sub>x</sub> films as the HTL in the reverse and forward scans.

HTL	Scan	J <sub>sc</sub> (mA/cm <sup>2</sup> )	V <sub>oc</sub> (V)	FF (%)	PCE (%)	HI
o-NiO <sub>x</sub>	Reverse	22.7	0.90	72	14.8	0.11
	Forward	22.1	0.99	65	13.0	
p-NiO <sub>x</sub>	Reverse	21.0	1.01	66	14.2	0.15
	Forward	21.0	0.94	59	12.1	
p-NiO <sub>x</sub> /o-NiO <sub>x</sub>	Reverse	21.5	1.01	75	15.6	0.09
	Forward	22.3	1.00	62	14.2	

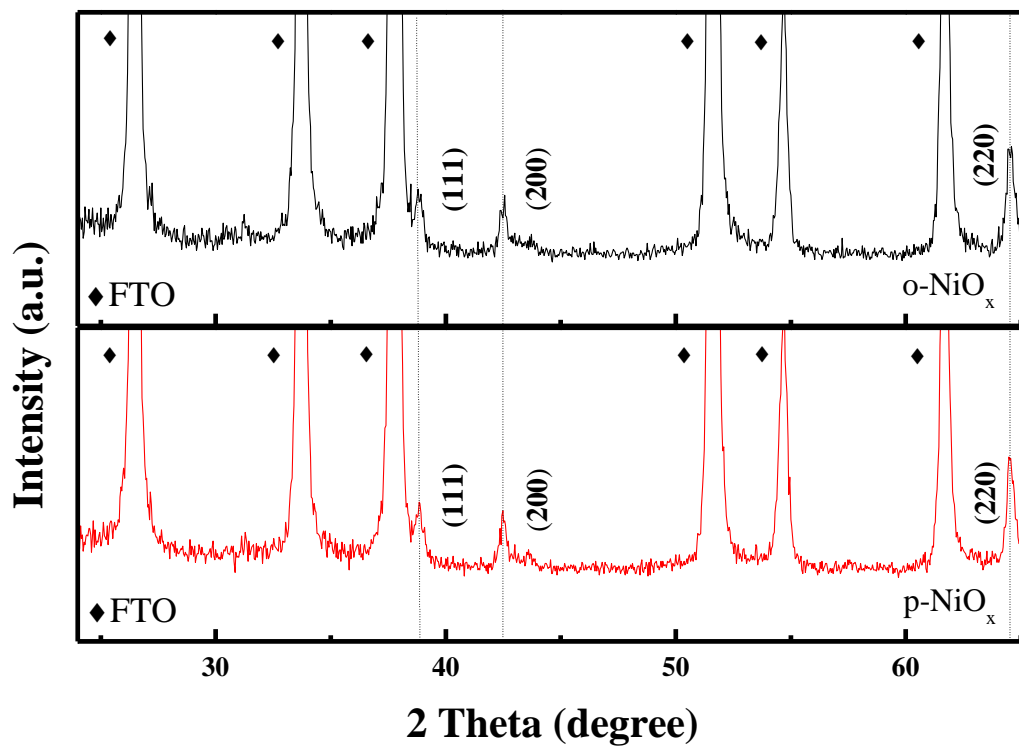


Figure S1. XRD patterns of the o-NiO<sub>x</sub> and p-NiO<sub>x</sub> films on the FTO substrates.

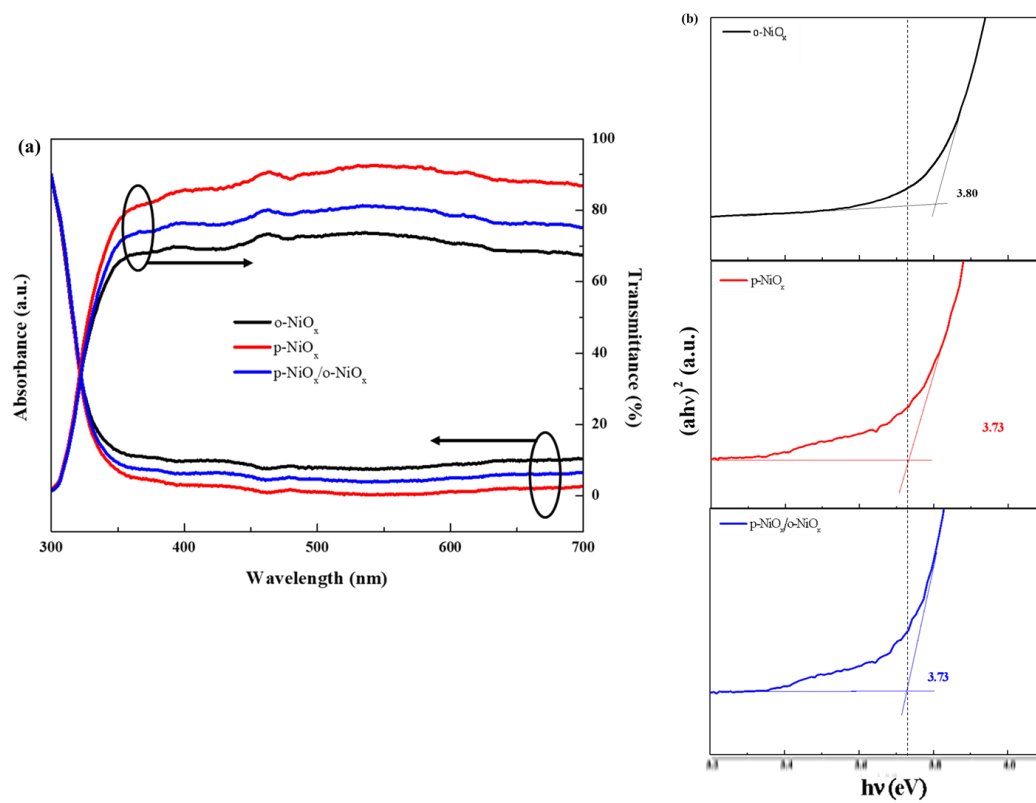


Figure S2. (a) Absorption and transmission spectra, (b) Tauc plots of the o-NiO<sub>x</sub>, p-NiO<sub>x</sub> and p-NiO<sub>x</sub>/o-NiO<sub>x</sub> films deposited on the FTO substrates.

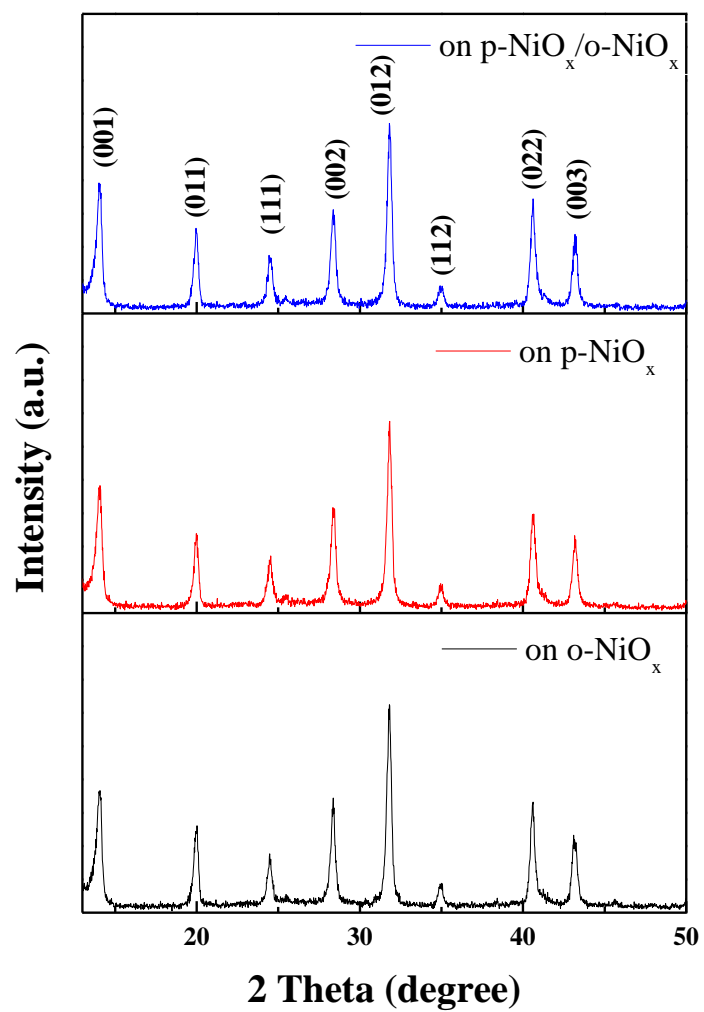


Figure S3. XRD patterns of perovskite layers on the o-NiO<sub>x</sub>, p-NiO<sub>x</sub> and p-NiO<sub>x</sub>/o-NiO<sub>x</sub> films.

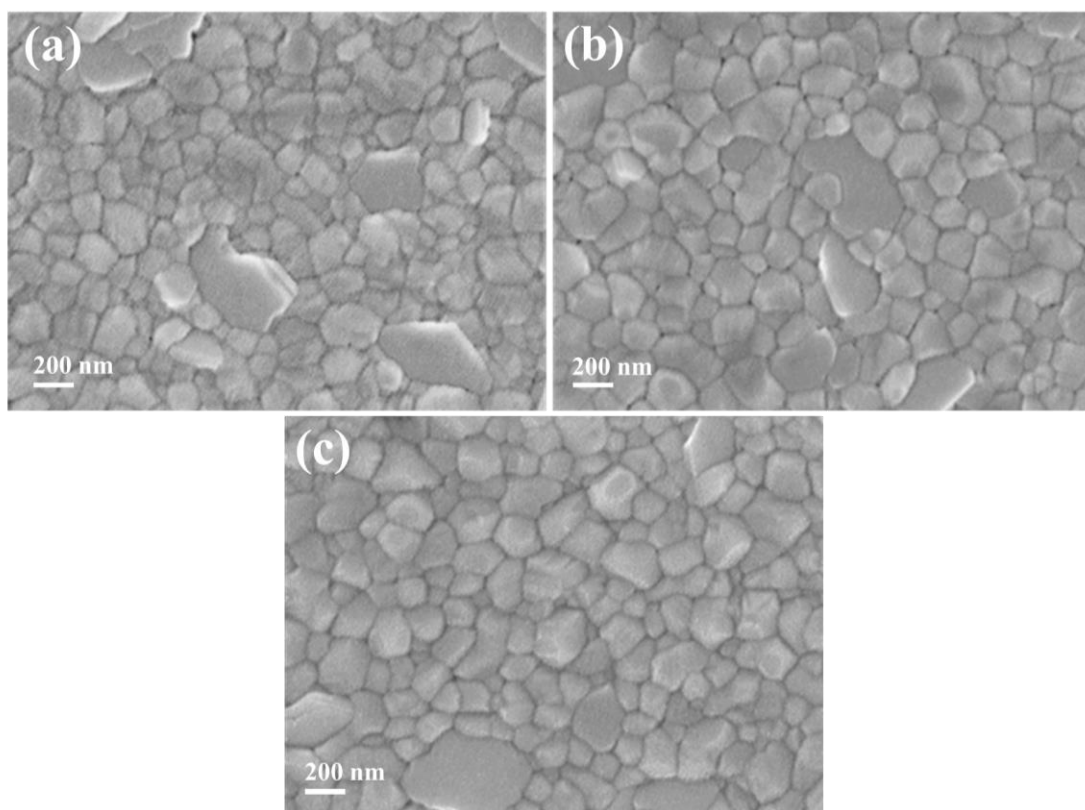


Figure S4. Top-view SEM images of perovskite layers on the (a) o-NiO<sub>x</sub>, (b) p-NiO<sub>x</sub>, and (c) p-NiO<sub>x</sub>/o-NiO<sub>x</sub> films.

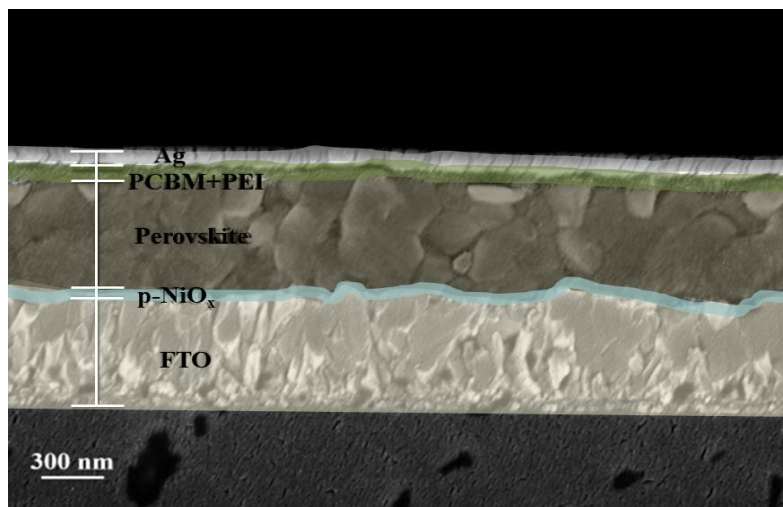


Figure S5. Cross-sectional SEM micrograph of the whole device with p-NiO<sub>x</sub>.

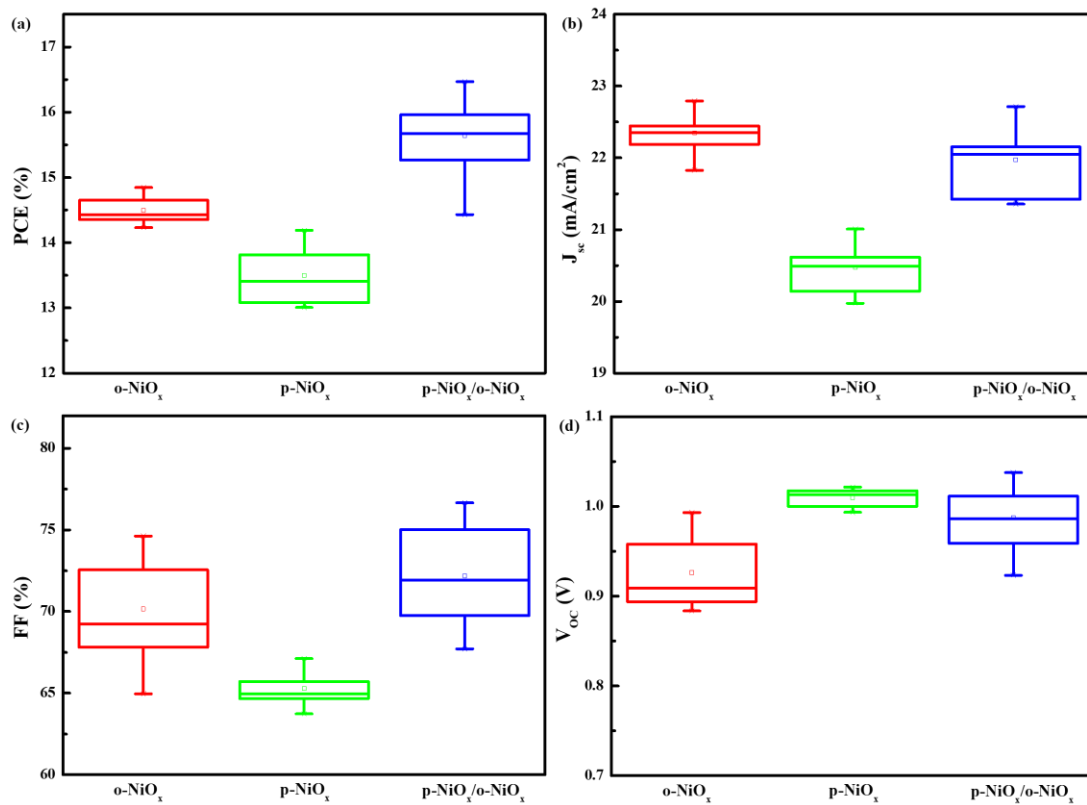


Figure S6. Performance variation is represented as a standard box plot in (a) PCE, (b) J<sub>sc</sub>, (c) FF, and (d) V<sub>oc</sub> from 20 devices based on the o-NiO<sub>x</sub>, p-NiO<sub>x</sub> and p-NiO<sub>x</sub>/o-NiO<sub>x</sub> films.

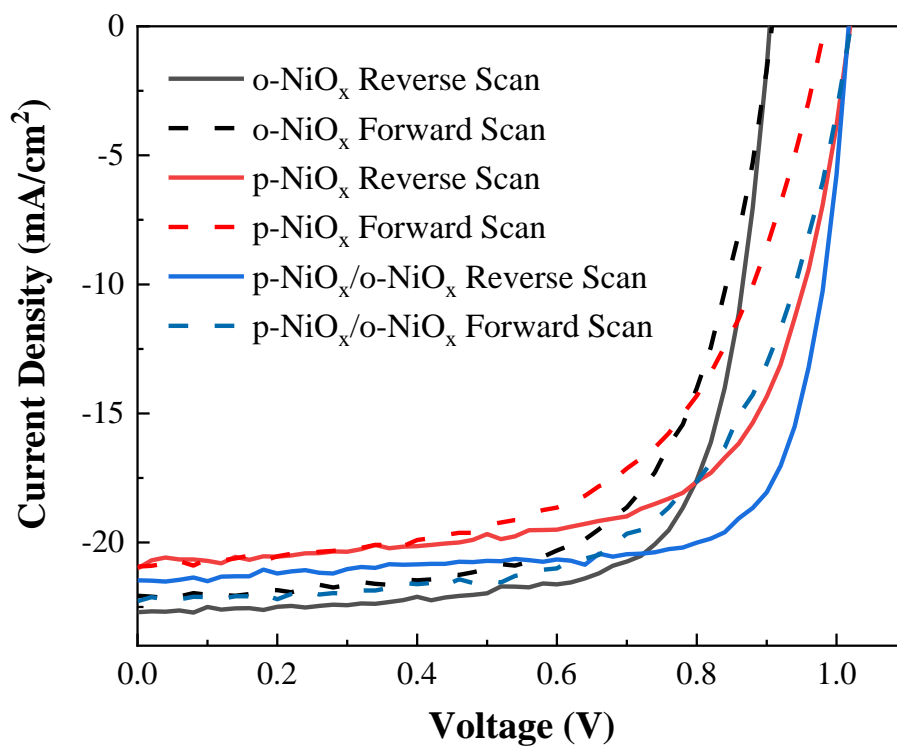


Figure S7. J–V characteristics of PSCs based on the o-NiO<sub>x</sub>, p-NiO<sub>x</sub> and p-NiO<sub>x</sub>/o-NiO<sub>x</sub> HTLs in the reverse and forward scans under AM 1.5G exposure.

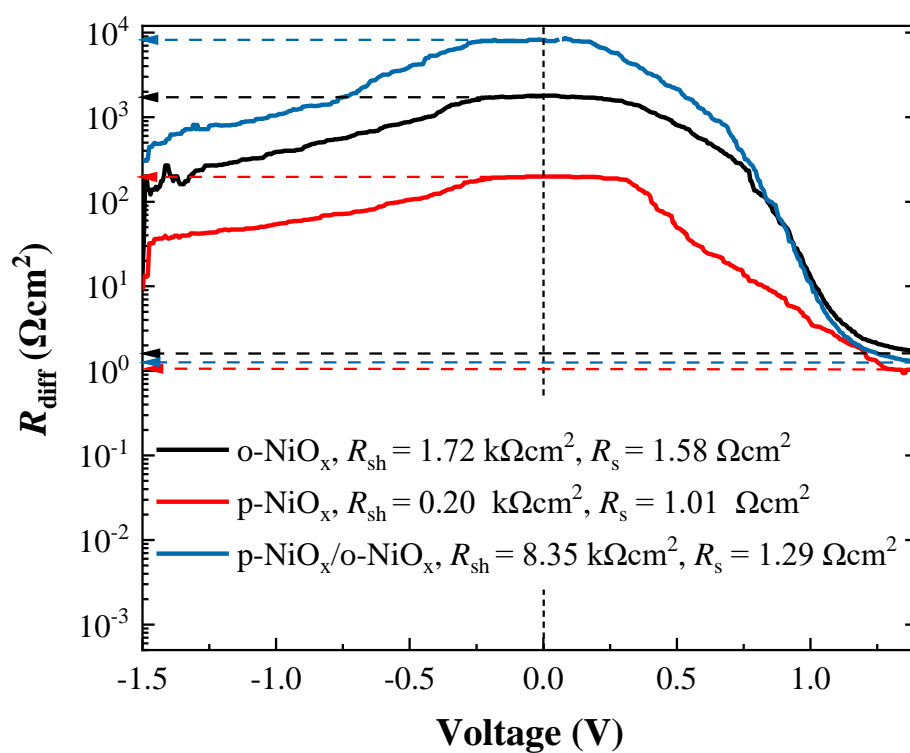


Figure S8. Differential resistance  $R_{\text{diff}}$  versus voltage of devices in the dark.